SCANNING VOL. 37, 429–437 (2015)

Useful Surface Parameters For Biomaterial Discrimination

Marina Etxeberria,[1] Tomas Escuin,[2] Miquel Vinas,[3] and Carlos Ascaso[4]

[1]Doctoral Student, Department of Dentistry and Department of Pathology and Experimental Therapeutics, Dentistry School, University of Barcelona, Barcelona, Spain
[2]Associate Professor, Laboratory of Prosthetic Dentistry, Dentistry School, University of Barcelona, Barcelona, Spain
[3]Department of Pathology and Experimental Therapeutics, Medical and Dentistry Schools, University of Barcelona, Barcelona, Spain
[4]Department of Public Health, Medical School, University of Barcelona, Barcelona, Spain

Summary: Topographical features of biomaterials' surfaces are determinant when addressing their application site. Unfortunately up to date there has not been an agreement regarding which surface parameters are more representative in discriminating between materials. Discs (n = 16) of different currently used materials for implant prostheses fabrication, such as cast cobalt-chrome, direct laser metal soldered (DLMS) cobalt-chrome, titanium grade V, zirconia (Y-TZP), E-glass fiber-reinforced composite and polyetheretherketone (PEEK) were manufactured. Nanoscale topographical surface roughness parameters generated by atomic force microscopy (AFM), microscale surface roughness parameters obtained by white light interferometry (WLI) and water angle values obtained by the sessile-water-drop method were analyzed in order to assess which parameter provides the best optimum surface characterization method. Correlations between nano-roughness, microroughness, and hydrophobicity data were performed to achieve the best parameters giving the highest discriminatory power. A subset of six parameters for surface characterization were proposed. AFM and WLI techniques gave complementary information. Wettability did not correlate with any of the nanoroughness parameters while it however showed a weak correlation with microroughness parameters. SCANNING 37:429–437, 2015. © 2015 Wiley Periodicals, Inc.

Key words: AFM, biomaterial, surface characterization, white light interferometry, wettability

Introduction

Surface features significantly condition many technological and biomedical applications of biomaterials (Ham and Powers, 2014). Surface roughness and surface wettability can significantly determine major aspects of biological interactions and, subsequently, allow to predict the eventual failure or success of an implant-prosthetic treatment (Park *et al*., 2012; Gittens *et al*., 2013). Surface modification strategies attempt to modulate the surface properties of biomaterials in order to affect cell-substrate interactions and improve the overall biological response (Ivanova *et al*., 2010). Furthermore, in order to accomplish this purpose a detailed characterization of surface topography must be achieved.

Characterization of surface roughness is complex as it depends on both the intrinsic properties of the material and manufacturing procedures and conditions (De Chiffre *et al*., 2000). In an attempt to have a more extensive and clear description, a wide variety of surface roughness parameters (RPs) have been developed. This has been termed as "the parameter rash" by Whitehouse (Whitehouse, 1982). Nevertheless, inconsistencies have been reported when describing surface topographies, in part due to the lack of standardized methods. Nowadays a wide set of parameters are being used; however, it seems that there is an urgent need to reduce the number of parameters in order to achieve a general standardization to facilitate comparisons and reduce cost.

Contract grant sponsor: Ajuts a la Recerca awarded to the School of Dentistry, University of Barcelona.

Marina Etxeberria DDS, MSc, (doctoral student) performed the specimen preparation, surface characterization, results analysis, and article writing (first and corresponding author).

*Address for reprints: Marina Etxeberria, Department of Dentistry, Dentistry School, University of Barcelona, Feixa Llarga s/n, 08907 Hospitalet de Llobregat, Barcelona, Spain.
E-mail: marinaetxebe@hotmail.com

Received 27 April 2015; revised 30 May 2015; Accepted with revision 4 June 2015

DOI: 10.1002/sca.21232
Published online 6 July 2015 in Wiley Online Library (wileyonlinelibrary.com).

The parameter reduction method is effective at selecting the RP to represent a surface (Nowicki, 1985; Rosén, 2008; Ham and Powers, 2014). This method is based on the analysis of strong and weak correlations between RPs; correlated RPs highlight the similarity between them; conversely, non-correlated RPs underline the difference among them. Highly correlated RPs are redundant and thereby one can be selected to represent the whole group. In contrast, poorly correlated RPs provide complementary information being thereby best discriminating between materials (Nowicki, 1985).

Progress in nanotechnologies has led to the development of nanometer resolution technologies allowing research and visualization at a scale in which interactions between bacterial cells and biomaterials' surfaces occur. Atomic Force Microscopy (AFM) is the most powerful tool for topographical characterization at the nanometer and sub-nanometer scales (Binnig *et al*., 1986; Dorobantu and Gray, 2010). AFM topography imaging is non-destructive and widely used in life sciences which provides high-resolution characterization of surface topography, biomolecules, membranes, and cells at the nanoscale. White Light Interferometry (WLI) is a type of computerized optical interference microscopy. Its use has rapidly widespread as a quality control of microscale engineering processes and has been used to analyze surface roughness and cell adhesion at the microscale (Hove *et al*., 2007). This method has been shown to be fast, non-destructive and accurate. The combination of both techniques has been proposed to improve the measuring efficiency of AFM for the surface characterization of biomaterials (Tyrrell *et al*., 2004; Guo *et al*., 2011).

To characterize surface structure, the present study examined six different dental materials for implant abutment manufacture using an atomic force microscope (AFM) for high resolution analysis, white light interferometry (WLI) and the drop-sessile-water method. From both methods for measuring surface roughness, amplitudinal roughness parameters were determined, which are so far the most cited surface parameters for surface characterization (Ivanova *et al*., 2010; Gittens *et al*., 2013; Webb *et al*., 2013). These are obtained from the height values of a given profile (denoted by R) or surface (denoted by S). The aim of this study was to attempt the combination of surface parameters resulting in an optimum surface description.

Materials and Methods

Specimen Preparation

Disks 10 mm in diameter and 2 mm thick were manufactured (n = 16) from six different implant abutment materials. The tested materials were: cast cobalt-chrome (Co–Cr), direct laser metal soldered (DLMS) Co–Cr disks, Titanium grade V disks, Zirconia (Y-TZP) disks, E-glass fiber-reinforced composite, and polyetheretherketone (PEEK). The disks were manufactured as previously described (Etxeberria *et al*., 2014).

Cast Cobalt-Chromium Disks

Acrylic resin (pattern resin® LS, GC Corp.) disks of the desired final shape were fabricated and casted by induction (Ducatron Série 3 UGIN'Dentaire. Seyssins. France) using Co-Cr (Wirobond C® alloy, BEGO, Bremer Goldschlägerei Wilh. Herbst GmbH and Co. KG, Bremen, Germany). After casting, the sprues were eliminated with the aid of carbide discs at low speed. The castings were sandblasted with 110 μm aluminum oxide particles (Korox®, Bego, Bremen, Germany) under three bar pressure to remove oxide films and residual investment.

DLMS Cobalt-Chromium Disks

The disk shaped specimens were designed in a 3D software package and saved in an industry standard stereolithography (STL) format. The standard DLMS (direct laser metal soldering) manufacturing method by EOSINT M 270 (EOSINT 270 GmbH Electro Optical Systems, Munich,Germany) was used to fabricate the disks.

Both the cast and the DLMS Co-Cr disks were polished in three stages: (a) using a hard rubber disk at 15,000 rpm; (b) then with a soft rubber disk at 15,000 rpm, and finally (c) using a soft brush with a polishing paste at 1400 rpm. Each polishing phase lasted 90 seconds.

Titanium Disks

Machined and polished titanium grade V disks were provided by Klockner® (Klockner–Soadco S.L., Andorra).

ZirconiaDisks

Zirconia (Y-TZP) disks were supplied by Dentisel (Dentisel S.L., Barcelona, Spain).

FRC Disks

E-glass FRC disks, prepared from rods, were provided by Bioloren® (Bioloren, S.r.L, Saronno, Varese, Italy).

PEEK Disks

Polyetheretherketone (PEEK) disks were obtained from rods and were supplied by Tekniimplant® (Tekniimplant S.L., Barcelona, Spain).

All disks were handled by their lateral walls not to damage the disks' surfaces. In addition were gently cleaned using a cotton pellet with ethanol and dried under warm dry air.

Characterization

Atomic force microscopy

The surface topographies of the tested materials were characterized at the nanoscale using AFM (XE-70, Park Systems, Korea). Images with the areas of $5 \times 5\ \mu m^2$ were scanned in the standard non-contact mode. The probe was supported on a rectangular-shaped cantilever tip (tip radius: < 10 nm, f$= \pm 300$ kHz, spring constant$= \pm 40$ N/m, silicon coating). The scan rate was 0.6 Hz and the resolution 256×256 pixels. Representative roughness parameters S_{Min}, S_{Max}, S_{Mid}, S_{Mean}, S_{pv}, S_q, S_a, S_z, S_{sk}, and S_{ku} described in Table I were calculated from the roughness values obtained by AFM and processed by XEI image processing software (Park Systems).

White Light Interferometry

The surface topographies of the tested materials were characterized at the microscale using a white light interferometer microscope (LeicaSCAN DCM3D, Leica Microsystems, Switzerland). A $50 \times$/0.50 Mirau objective was utilized. The threshold was set to 1.0% and the Gaussian filter to 25 μm. Vertical scanning interferometry mode images with the areas of $250.64 \times 190.90\ \mu m^2$ were obtained. Image data-analyses were performed using Leica map DCM 3D, version 6.2.6561 (Leica Microsystems, Switzerland) and R_p ,R_v, R_z, R_t, R_a, R_q, S_a, S_z, and S_q roughness parameters described in Table I were calculated.

Surface Wettability

External water contact angles were analyzed with the sessile-water-drop method at room temperature (Truong *et al*., 2010; Gittens *et al*., 2013). A 10 μL drop of MilliQ–quality water was placed onto the center of each specimen using an injector. Digital photographs were taken (Nikon D70) and the determination of the external contact angle was done using IMAT software (CCIT, Barcelona, Spain). Two contact angles (θ_{left} and θ_{right}) per disk were obtained.

Statistical Analysis

The surface nanoroughness, microroughness and wettability data did not follow a normal distribution. Therefore, a non-parametric ANOVA statistical analysis was carried out for data comparisons. Quantitative data analysis including the median, minimum, and

TABLE I Summary of roughness parameters (Stout et al., 1994).

Surface characterization technique	Symbol	Parameter
Atomic force microscopy	S_{max}	Maximum height of the surface
	S_{min}	Minimum height of the surface
	S_{mid}	Median height of the surface
	S_{mean}	Mean height of the surface
	S_{pv}	Peak to valley height
	S_a	Arithmetical mean deviation of surface roughness
	S_q	Root-mean-square deviation of surface topography
	S_z	Ten point height of surface topography
	S_{sk}	Skewedness of topography height distribution
	S_{ku}	Kurtosis of topography height distribution
White light interferometry	S_a	Arithmetical mean deviation of surface roughness
	S_z	Ten point height of surface topography
	S_q	Root-mean-square deviation of surface topography
	R_p	Maximum peak height of the roughness profile
	R_v	Maximum valley depth of the roughness profile
	R_z	Ten point height of the roughness profile
	R_t	Total height of the roughness profile
	R_a	Arithmetical mean deviation of the roughness profile
	R_q	Root-mean-square deviation of the roughness profile
Wettability	θ_{left}	Left contact angle
	θ_{right}	Right contact angle

maximum were computed for each parameter. Spearman's rank correlation coefficient was used to express the degree of pair-wise association among nanoroughness parameters, microroughness parameters, and wettability. In order to identify statistical differences among the materials, Kruskal–Wallis and Mann–Whitney U test were performed with the Bonferroni adjustment according to the number of tests performed. Total data were analyzed in SPSS 21.0 to provide descriptive statistics and to perform non-parametric testing. Statistical analysis was performed with Statistical Package for the Social Sciences (Version 21.0; SPSS., Inc, Chicago, Illinois). Hypotheses were contrasted with an alpha error of 5% and estimations with 95% confidence level.

Results

Overall results of the measurements on the surfaces are summarized in Tables II–IV. Tables II, III and IV describe the median, minimum and maximum values computed for each surface parameter carried out of 16 estimations per each material.

Correlation coefficient calculations are presented from Table V to Table VII : among nanoscale roughness parameters and wettability (Table V); among microscale roughness parameters and wettability (Table VI) and finally Table VII summarizes the correlations between nanoscale and microscale roughness parameters. At the nanoscale, roughness parameters showed poor correlations however three clusters of parameters are differentiated. A highly correlated group ($r>0.86$) comprised by S_a-S_{max}-S_{min}-S_{pv}-S_q-S_z in addition to S_{mean}-S_{mid} and S_{sk}-S_{ku} groups that are weakly correlated ($r = 0.29$ and $r = -0.32$ respectively) among themselves. Contrary to the nanoscale, at the microscale all the parameters are correlated ($r>0.58$). Nevertheless, two subgroups are slightly differently related by their correlation degree: the profile roughness parameters and the surface roughness parameters. Contact angles (θ_{left} and θ_{right}) are highly correlated ($r = 0.97$) among themselves regardless of the scale. Wettability did not correlate with any of the nanoroughness parameters in contrast it showed a weak and negative correlation with microroughness parameters. Correlation analysis of nano and microescale parameters in Table VII presented few and weak correlations.

Results of Kruskal–Wallis ($p<0.01$) and Mann–Whitney U test ($p<0.003$) (Tables II, III) show that S_a roughness parameter exhibited the highest discrimination power at both scales.

Characterization of the Tested Materials

Results of the characterization of the analyzed materials showed that FRC was found to be the roughest

TABLE II Median, minimum, and maximum values of nanoscale surface parameters in nanometres. Results of Kruskal–Wallis (p-value) and Mann–Whitney U-test with Bonferroni correction (number of pairs of materials with statistically significant differences)

	Cast Co-Cr	DLMS Co-Cr	Titanium	Zirconia	FRC	PEEK	Kruskal–Wallis p*	Different pairs**
S_{min}	−200.5 (−494; −57)	−69 (−411; −25)	−125 (−181; −75)	−355 (−573; 258)	−507 (−993; −1)	−207 (−515; −85)	0.03	0
S_{max}	178 (51; 633)	80.5 (32; 502)	143 (82; 201)	427 (1; 759)	253 (1; 980)	194 (110; 591)	0.2	0
S_{mid}	−2 (−157; 69)	8.5 (−45; 140)	15.5 (−36; 32)	30.5 (−89; 164)	0.0 (−127; 141)	−6 (−67; 199)	0.1	0
S_{mean}	0.0 (−82; −0)	0.0 (0.0; 0.0)	0.0 (0.0; 0.0)	0.0 (0; −134)	0.0 (0.0; 0.0)	0.0 (0; −152)	0.4	0
S_{pv}	427 (128; 112)	183.5 (64; 91)	265.5 (189; 37)	795.5 (1; 1297)	761 (2; 1860)	457 (221; 932)	0.01	4
S_a	53.5 (11; 142)	11.5 (4; 132)	32 (22; 31.5)	99.5 (0; 185)	87 (0; 268)	42.5 (17; 167)	0.01	6
S_q	66 (14; 179)	19 (6; 153)	32 (22; 66)	128 (0; 234)	114 (0; 329)	61 (22; 184)	0.01	4
S_z	421 (106; 1126)	179 (61; 906)	259 (182; 363)	787.5 (1; 1276)	750 (2; 1825)	445 (216; 920)	0.01	4
S_{sk}	0 (−1; 1)	0 (−7; 2)	0 (−1; 1)	0 (−1; 0)	0 (0; 1)	0 (−1; 1)	0.6	1
S_{ku}	3.5 (2; 7)	5 (2; 71)	3 (2; 9)	3 (2; 5)	3 (2; 6)	4 (2; 11)	0.03	1

*Statistically significant differences $p < 0.01$.
**Different pairs of materials as determined by Mann–Whitney U-test $p < 0.003$.

TABLE III Median, minimum, and maximum values of microscale surface parameters. Results of Kruskal–Wallis (p-value) and Mann–Whitney U-test with Bonferroni correction (number of pairs of materials with statistically significant differences)

	Cast Co-Cr	DLMS Co-Cr	Titanium	Zirconium	FRC	PEEK	Kruskal-Wallys p*	Different pairs**
S_a	0.15 (0.04; 0.18)	0.06 (0.01; 0.18)	0.08 (0.08; 0.63)	0.15 (0.11; 0.30)	0.87 (0.34; 1.33)	0.22 (0.18; 0.32)	<0.01	11
S_z	2.44 (0.54; 18.1)	1.83 (0.31;104.14	1.19 (0.88; 5.46)	2.83 (1.87; 8.08)	24.71 (12.5; 108.41)	4.37 (3.4; 12.78)	<0.01	8
S_q	0.21 (0.44; 0.23)	0.21 (0.02; 0.63)	0.11 (0.08, 0.16)	0.21 (0.14; 0.41)	1.31 (0.53; 1.92)	0.31 (0.24; 0.47)	<0.01	8
R_p	0.17 (0.02; 0.29)	0.06 (0.02; 0.23)	0.12 (0.04; 0.32)	0.29 (0.18; 0.73)	1.26 (0.30; 4.26)	0.22 (0.11; 0.57)	<0.01	10
R_v	0.21 (0.00; 0.47)	0.12 (0.03; 0.33)	0.14 (0.03; 0.30)	0.25 (0.14; 0.50)	1.40 (0.41; 3.26)	0.21 (0.00; 0.59)	<0.01	7
R_z	0.41 (0.00; 0.76)	0.19 (0.05; 0.56)	0.27 (0.08; 0.50)	0.54 (0.33; 1.14)	2.64 (0.72; 7.10)	0.45 (0.00; 1.17)	<0.01	8
R_t	0.66 (0.16; 1.45)	0.37 (0.10; 0.94)	0.41 (0.20;1.80)	0.88 (0.56; 3.36)	5.42 (3.49; 25.51)	1.07 (0.48; 2.23)	<0.01	9
R_a	0.07 (0.01; 0.01)	0.03 (0.00; 0.11)	0.05 (0.13; 0.10)	0.10 (0.68; 0.20)	0.51 (0.11; 1.07)	0.11 (0.04; 0.24)	<0.01	9
R_q	0.10 (0.01; 0.18)	0.04 (0.01; 0.13)	0.06 (0.83; 0.13)	0.13 (0.00; 0.27)	0.69 (0.15; 1.48)	0.13 (0.05; 0.30)	<0.01	9

*Statistically significant differences $p < 0.01$.
**Different pairs of materials as determined by Mann–Whitney U-test $p < 0.003$.

while DLMS Co-Cr resulted the smoothest. Zirconia was shown to be the most hydrophilic whereas FRC resulted the most hydrophobic material. Finally, in Figure 1 a graphic representation of the discrimination of the materials according to the selected parameters is described.

Discussion

Several attempts have been made to establish a set of surface parameters giving the optimum surface description for the discrimination of materials (Stout *et al*., 1994; Crawford *et al*., 2012; Webb *et al*., 2013). However, the statistical dependence of the surface parameters has rarely been analyzed. The present study is in agreement with previous studies that state that the commonly used parameters to characterize biomaterials are redundant (Stout *et al*., 1994; Crawford *et al*., 2012; Webb *et al*., 2013). A set of six parameters giving the highest discriminatory power (S_a,$S_{ku,}$ and S_{mid} at the nanoscale, S_a and S_z at the microscale and θ_{right}) where selected out of 21 parameters to represent the whole group of parameters.

The poor correlations exhibited among the nanoscale surface parameters are in agreement with previous studies (Rosén *et al*., 2008). However the strong correlations displayed by the S_a-S_{max}-S_{min}-S_{pv}-S_q-S_z cluster of parameters means that the determination of one of the parameters automatically leads to the definition of the others. S_{mean}-S_{mid} and S_{sk}-S_{ku} groups are not correlated thereby they provide additional complementary information. The present results may be explained by the fact that all the highly correlated parameters are height descriptors, S_{mean}, S_{mid} are normality height descriptors and S_{sk}, S_{ku} describe the spatial surface topography. Regarding the most correlated group, the criteria for selecting the parameter to represent the group was based on the most sensitive parameter in the materials discrimination which was

TABLE IV Median, minimum, and maximum values of external contact angle measurements. Results of Kruskal–Wallis (p-value) and Mann–Whitney U-test with Bonferroni correction (number of pairs of materials with statistically significant differences)

	Cast Co-Cr	DLMS Co-Cr	Titanium	Zirconia	FRC	PEEK	Kruskal–Wallis p*	Different pairs**
θ_{left}	91.1 (78.6; 117)	95.8 (78.8; 106.3)	88.3 (73; 111.6)	110.2 (80.1; 124.3)	75.3 (50.8; 114)	93.5 (70.3; 103.4)	0.001	3
θ_{right}	91.6 (80.2; 115.2)	93.6 (77.4; 109.5)	89.8 (73; 115.7)	108.2 (81.1; 122.2)	74.5 (51.1; 109)	92.8 (70.9; 100.1)	0.0	4

*Statistically significant differences $p < 0.01$.
**Different pairs of materials as determined by Mann–Whitney U-test $p < 0.003$.

TABLE V Correlation matrix showing correlation coefficients (r values) for nanoscale roughness parameters and wettability

	S_{min}	S_{max}	S_{mid}	S_{mean}	S_{pv}	S_q	S_a	S_z	S_{sk}	S_{ku}	θ_{left}
S_{max}	−0.86**										
S_{mid}	0.09	0.26*									
S_{mean}	−0.02	0.20*	0.29**								
S_{pv}	−0.94**	0.96**	0.07	0.10							
S_q	−0.91**	0.92**	0.04	0.10	0.96**						
S_a	−0.90**	0.90**	0.03	0.10	0.94**	0.99**					
S_z	0.18	0.96**	0.08	0.10	1.00**	0.96**	0.94**				
S_{sk}	−0.18	−0.10	−0.53**	−0.09	0.05	0.15	0.17	0.05			
S_{ku}	0.07	−0.01	0.16	−0.09	−0.06	−0.23*	−0.27**	−0.06	−0.32**		
θ_{left}	0.06	−0.06	−0.11	−0.08	−0.05	−0.05	−0.06	−0.04	−0.02	0.02	
θ_{right}	0.05	−0.05	−0.08	−0.08	−0.04	−0.04	−0.04	−0.04	0.03	0.03	0.97**

** $p < 0.01$.
* $p < 0.05$.

found to be S_a (Table II). From the less correlated groups, the criteria for selecting the parameter was the lesser correlation of parameters. Hence, a preliminary set of three independent parameters, S_a, S_{mid}, and S_{ku} was selected.

S_a (or its counterpart R_a) is one of the most commonly used parameters to quantify surface topography (Whitehead *et al*., 2005; Truong *et al*., 2010; Crawford *et al*., 2012). It quantifies the "absolute" magnitude of surface heights but in contrast, is insensitive to the spatial distribution of the heights. Similarly to previous studies, our results highlight that the S_a value is insufficient for the surface discrimination of biomaterials at the nanoscale and spatial surface descriptors are needed for an optimized surface characterization (Ivanova *et al*., 2010; Webb *et al*., 2012). In practical terms, kurtosis values describe the shape of the distribution of the heights; (i.e., normal distributions have kurtosis value of three while sharper distributions have higher values and rounded distributions have lower). In the present study, DLMS Co-Cr and PEEK showed the smoothest surfaces at the nanoscale obtaining kurtosis values > 3 compared to the rest of materials, which had values of < 3. On the other hand, the zero value for S_{sk}, (skewedness is a measure of the symmetry of height distribution) reflects symmetrical height distribution and these results are corroborated by a zero value for S_{mean}. This may be explained by the fact that the materials underwent polishing procedures. It is evident that these parameters (kurtosis and skewedness) are material-dependent and that either one or the other or both should be addressed depending on the required information (Crawford *et al*., 2012). To the authoŕs knowledge, S_{mid} has not been addressed before.

The applicability of the first subset of parameters has also played a role in determining bacterial adhesion. Thereby, in the study of Webb et al. the S_a, S_q, and S_{max} parameters gathered similar bacterial counts in contrast to S_{sk} and S_{ku} (Webb *et al*., 2013).

In contrast to the nanoscale, at the microscale, all the roughness parameters are correlated (Table V) nevertheless, profile values are slightly differently related by

TABLE VI Correlation matrix showing correlation coefficients (r values) for microscale roughness parameters and wettability

	S_a	S_z	S_q	R_p	R_v	R_z	R_t	R_a	R_q	θ_{left}
S_z	0.75**									
S_q	0.94**	0.87**								
R_p	0.84**	0.65**	0.77**							
R_v	0.69**	0.58**	0.66**	0.85**						
R_z	0.81**	0.65**	0.75**	0.95**	0.93**					
R_t	0.84**	0.71**	0.79**	0.88**	0.78**	0.99**				
R_a	0.87**	0.65**	0.79**	0.96**	0.88**	0.96**	0.88**			
R_q	0.85**	0.66**	0.79**	0.96**	0.87**	0.96**	0.89**	0.99**		
θ_{left}	−0.22*	−0.19	−0.21*	−0.18	−0.25*	−0.24*	−0.28**	−0.22**	−0.22**	
θ_{right}	−0.26*	−0.23*	−0.26*	−0.19	−0.25*	−0.25	−0.29*	−0.24*	−0.24*	0.97**

** $p < 0.01$.
* $p < 0.05$.

TABLE VII Correlation matrix showing correlation coefficients (r values) for microscale and nanoscale roughness parameters

	S_a	S_z	S_q	R_p	R_v	R_z	R_t	R_a	R_q
S_{min}	−0.31**	−0.21	−0.25*	−0.27**	−0.18	−0.25*	−0.19	−0.28**	−0.27**
S_{max}	0.23*	0.15	0.23*	0.23*	0.17	0.21*	0.16	0.23*	0.22*
S_{mid}	−0.15	−0.16	−0.10	−0.04	−0.03	−0.04	−0.07	−0.07	−0.07
S_{mean}	0.06	0.03	0.06	0.04	0.03	0.04	0.15	0.03	0.03
S_{pv}	0.29**	0.20	0.27**	0.27**	0.19	0.25*	0.20	0.28**	0.27*
S_q	0.25*	0.14	0.21*	0.24*	0.16	0.20	0.19	0.23*	0.22*
S_a	0.21	0.09	0.16	0.21*	0.13	0.17	0.16	0.20	0.19
S_z	0.29**	0.19	0.27**	0.28**	0.19	0.25*	0.20	0.28**	0.27*
S_{sk}	0.07	0.09	0.02	0.06	0.10	0.07	0.16	0.07	0.08
S_{ku}	−0.24*	−0.02	−0.15	−0.17	−0.12	−0.09	−0.20	−0.15	−0.13

** $p < 0.01$.
* $p < 0.05$.

their correlation degree to surface values. These findings are comparable to previous studies (Nowicki, 1985; Rosén *et al*., 2008; Ham and Powers, 2014) however, the different correlation values obtained by Ham et al. is due to the different averaging methods. In their study the mean of three calculations was computed while in ours the median of 16 calculations. Due to the fact that all the parameters are correlated, the selection of the best set of roughness parameter for is hindered. Therefore, S_a was selected to represent the whole group of parameters for being the most sensitive parameter on the pair-wise material discrimination at the microscale (Table III).

This result is confirmed by recent studies which recommended the selection of S values as they are obtained from the surface and thus are more representative compared to those obtained from the profile (Webb *et al*., 2013). In the present study, S_z shows the lowest correlation value with S_a and with the rest of parameters and thus could be considered as a useful complementary roughness parameter. The efficiency of both parameters determined as the average and the maximum values has been widely used for material discrimination (Gorlenko *et al*., 1981; Nowicki, 1985; Gittens *et al*., 2013). Thus at the microscale subset, the two selected parameters are S_a and S_z.

The few and weak correlations encountered among nano and microroughness (Table VII) suggest that both techniques give complementary information and thus it

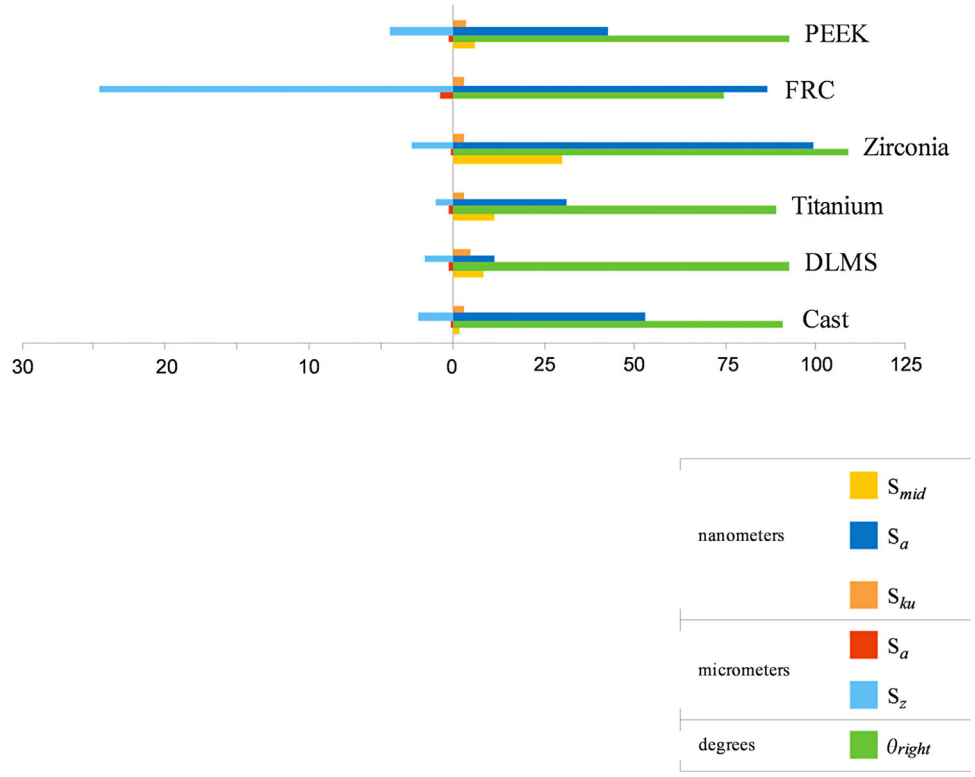

Fig. 1. Characterization of the materials according to the selected parameters.

is of paramount concern to include two different scales. These results are in agreement with previous authors' recommendations of using optical measuring methods such as white light interferometry to expand the AFM measuring range and to improve roughness measuring efficiency (Tyrrell *et al*., 2004; Guo *et al*., 2011). Therefore, in general S_a-S_{ku}-S_{mid} at the nanoscale and S_a-S_z at the microscale are not correlated being confirmed the complementarity of both groups of parameters.

As first described by Wenzel, an intimate relationship between surface roughness and wettability exists (Wenzel, 1949). Nevertheless, this correlation was not observed at the nanoscale. Likewise in a recent study, no correlation was found between roughness and wettability at the nanoscale (Gittens *et al*., 2013). While wettability values did not correlate with nanoroughness parameters, they correlated poorly with microroughness parameters. The negative correlation encountered indicates that as the roughness value increases the external angle contact value decreases and vice versa. This is explained by Wenzel's method that states that roughness induces hydrophobicity (Wenzel, 1949) and has been confirmed in previous studies (Gittens *et al*., 2011; Webb *et al*., 2013).

The selected parameters are efficient in characterizing and differentiating between materials and the obtained characterizations are in agreement with previous studies (Rosentritt *et al*., 2009; Ivanova *et al*., 2010; Adbulmajeed *et al*., 2014; Ourahmoune *et al*., 2014; Kim *et al*., 2015). FRC exhibited the highest roughness value among the tested materials values but in the range of previous studies (Tanner *et al*., 2003; Garoushi *et al*., 2009; Adbulmajeed *et al*., 2014). In contrast, DLMS Co-Cr obtained the lowest roughness value. This finding is in agreement with recent studies that support the notion that the powder additive manufacturing layer by layer improves the surface compared to the conventional casting methods (Oyagüe *et al*., 2012; Castillo-Oyagüe *et al*.,2013). However, this finding is not in accordance with a recent study where the average roughness value of DLMS was significantly higher compared to cast Co-Cr. One explanation could be differences in the composition of the used metal alloys (Kilicarslan and Ozcan, 2012).

Previous studies have shown that smooth microscale surface characteristics (R_a less than 0.1 μm) have minor influence on the surface wettability of a surface (Busscher *et al*., 1994; Adbulmajeed *et al*., 2011). In those studies smooth surfaces displayed contact angles that ranged between 60° and 86° and the differences of the contact angles were related to the surface chemistry. The present study, is in agreement with those studies since all the smooth surfaces investigated (all the materials except for FRC) showed contact angle values within this given range. Accordingly, rough FRC surfaces showed a contact angles above 86° showing a similarity in the trend claimed by Wenzel (Wenzel, 1949). Wettability values in general are also in agreement with previous studies except for the Zirconia which showed the highest contact angle value. This may be explained by the fact that the surfaces were rougher than in previous studies (Att *et al*., 2009). On the other hand, FRC showed the lowest wettability, which may be explained by the influence of fibers on the wettability behavior of composite materials (Adbulmajeed *et al*., 2014).

The limitations of measuring devices may introduce errors during data acquisition which may reflect on the final surface characterization. For instance, even the very sharp tip of an AFM shows limitations, and the optical methods are limited when recording small wavelength components. In addition to this, filtering techniques should be considered with care.

Correlation tests can be carried out to systematize the choice of a set of parameters when multiple parameters have to be reduced. The selection of parameters should be founded on the results of the degree of correlation between the multiple parameters and the required properties regarding their application site. This set of parameters was efficient in differentiating between six types of materials at the nano and microscale. The adoption of this proposed set of parameters will enable universal comparisons.

Conclusions

The present study proposes six parameters for characterizing biomaterial surfaces:

S_a-S_{ku}-S_{mid} at the nanoscale, S_a-S_z at the microscale and one angle contact value are suggested for surface characterization.

Roughness quantification at two different scales gave complementary information.

Wettability was not correlated with nanoroughness. In contrast, it was correlated with rough surfaces at the microscale.

References

Abdulmajeed AA, Walboomers XF, Massera J, et al. 2014. Blood and fibroblast responses to thermoset BisGMA-TEGDMA/glass fiber-reinforced composite implants in vitro. Clin Oral Implants Res 25:843–851.

Abdulmajeed AA, Lassila LV, Vallittu PK, Närhi TO. 2011. The effect of exposed glass fibers and particles of bioactive glass on the surface wettability of composite implants. Int J Biomater DOI: 10.1155/2011/607971.

Att W, Takeuchi M, Suzuki T, et al. 2009. Enhanced osteoblast function on ultraviolet light-treated zirconia. Biomaterials 30:1273–1280.

Binnig G, Quate CF, Gerber C. 1986. Atomic force microscope. Phys Rev Lett 56:930–933.

Busscher HJ, Van Pelt AWJ, De Boer P, De Jong HP, Arends J. 1984. The effect of surface roughening of polymers on

measured contact angles of liquids. Colloids and Surf 9: 319–331.
Castillo-Oyagüe R, Lynch CD, Turrión AS, López-Lozano JF, et al. 2013. Misfit and microleakage of implant-supported crown copings obtained by laser sintering and casting techniques, luted with glass-ionomer, resin cements and acrylic/urethane-based agents. J Dent 41:90–96.
Crawford RJ, Webb HK, Truong VK, Hasan J, Ivanova EP. 2012. Surface topographical factors influencing bacterial attachment. Adv Colloid Interface Sci 179-182 142–149.
De Chiffre L, Lonardo P, Trumpold H, et al. 2000. Quantitative characterisation of surface texture. CIRP Annals-Man Tech 49:635–652.
Dong WP, Sullivan PJ, Stout KJ. 1994. Comprehensive study of parameters for characterising three-dimensional surface topography: III: Parameters for characterizing amplitude and some functional properties. Wear 178:29–43.
Dorobantu LS, Gray MR. 2010. Application of atomic force microscopy in bacterial research. Scanning 32:74–96.
Etxeberria M, López-Jiménez L, Merlos A, Escún T, Viñas M. 2013. Bacterial adhesion efficiency on implant abutments: A comparative study. Int Microbiol 16:235–242.
Gittens RA, McLachlan T, Olivares-Navarrete R, et al. 2011. The effects of combined micron-/submicron-scale surface roughness and nanoscale features on cell proliferation and differentiation. Biomaterials 32:3395–3403.
Gittens RA, Olivares-Navarrete R, Cheng A, et al. 2013. The roles of titanium surface micro/nanotopography and wettability on the differential response of human osteoblast lineage cells. Acta Biomater 9:6268–6277.
Gorlenko OA 1981. Assessment of surface roughness parameters and their interdependence. Precis Eng 3:105–108.
Guo T, Wang S, Dorantes-Gonzalez DJ, et al. 2011. Development of a hybrid atomic force microscopic measurement system combined with white light scanning interferometry. Sensors 12:175–188.
Ham M, Powers BM. 2014. Roughness parameter selection for novel manufacturing processes. Scanning 36:21–29.
Hove LH, Holme B, Young A, Tveit AB. 2007. The erosion-inhibiting effect of TiF4, SnF2, and NaF solutions on pellicle-covered enamel in vitro. Acta Odontol Scand 65:259–264.
Ivanova EP, Truong VK, Wang JY, et al. 2010. Impact of nanoscale roughness of titanium thin film surfaces on bacterial retention. Langmuir 26:1973–1982.
Kilicarslan MA, Ozkan P. 2012. Evaluation of retention of cemented laser-sintered crowns on unmodified straight narrow implant abutments. Int J Oral Maxillofac Implants 28:381–387.
Kim YS, Shin SY, Moon SK, Yang SM. 2015. Surface properties correlated with the human gingival fibroblasts attachment on various materials for implant abutments: A multiple regression analysis. Acta Odontol Scand 73:38–47.
Lassila LV, Garoushi S, Tanner J, Vallittu PK, Söderling E. 2009. Adherence of Streptococcus mutans to Fiber-Reinforced Filling Composite and Conventional Restorative Materials. Open Dent J 4:227–232.
Nowicki B 1985. Multiparameter representation of surface roughness. Wear 102:161–176.
Ourahmoune R, Salvia M, Mathia TG, Mesrati N. 2014. Surface morphology and wettability of sandblasted PEEK and its composites. Scanning 36:64–75.
Oyagüe RC, Sánchez-Turrión A, López-Lozano JF, et al. 2012. Evaluation of fit of cement-retained implant-supported 3-unit structures fabricated with direct metal laser sintering and vacuum casting techniques. Odontology 100:249–253.
Park JH, Wasilewski CE, Almodovar N, et al. 2012. The responses to surface wettability gradients induced by chitosan nanofilms on microtextured titanium mediated by specific integrin receptors. Biomaterials 33:7386–7393.
Rosén BG, Anderberg C, Ohlsson R. 2008. Parameter correlation study of cylinder liner roughness for production and quality control. Proceedings of the Institution of Mechanical Engineers. Part B: J Eng Manuf 222:1475–1487.
Rosentritt M, Behr M, Bürgers R, Feilzer AJ, Hahnel S. 2009. In vitro adherence of oral streptococci to zirconia core and veneering glass-ceramics. J Biomed Mater Res B Appl Biomaterials 91:257–263.
Tanner J, Carlén A, Söderling E, Vallittu PK. 2003. Adsorption of parotid saliva proteins and adhesion of Streptococcus mutans ATCC 21752 to dental fiber-reinforced composites. J Biomed Mater Res B Appl Biomater 15:391–398.
Truong VK, Lapovok R, Estrin YS, et al. 2010. The influence of nano-scale surface roughness on bacterial adhesion to ultrafine-grained titanium. Biomaterials 31:3674–3683.
Tyrrell JW, Dal Savio C, Krüger-Sehm R, Danzebrink HU. 2004. Development of a combined interference microscope objective and scanning probe microscope. Rev Sci Inst 75:1120–1126.
Webb HK, Boshkovikj V, Fluke CJ, et al. 2013. Bacterial attachment on sub-nanometrically smooth titanium substrata. Biofouling 29:163–170.
Webb HK, Truong VK, Hasan J, et al. 2012. Roughness parameters for standard description of surface nanoarchitecture. Scanning 34:257–263.
Whitehead KA, Colligon J, Verran J. 2005. Retention of microbial cells in substratum surface features of micrometer and sub-micrometer dimensions. Colloid Surf B Biointerfaces 41:129–138.
Whitehouse DJ 1982. The parameter rash—is there a cure?. Wear 83:75–78.
Wenzel RN. 1949. Surface roughness and contact angle. J Phys Colloid Chem 53:1466–1467.